Surface-Induced Crystal Orientation of Poly(trimethylene 2,6-naphthalate) Films Studied by Polarized FTIR-ATR and Grazing Incidence X-ray Diffraction

ARTICLE *in* MACROMOLECULES · OCTOBER 2005

Impact Factor: 5.8 · DOI: 10.1021/ma051651o

2 AUTHORS:

Yongri Liang
Beijing Institute of Petrochemical Technology
46 PUBLICATIONS **408** CITATIONS
SEE PROFILE

Han Sup Lee
Inha University
33 PUBLICATIONS **534** CITATIONS
SEE PROFILE

Surface-Induced Crystal Orientation of Poly(trimethylene 2,6-naphthalate) Films Studied by Polarized FTIR-ATR and Grazing Incidence X-ray Diffraction

Yongri Liang and Han Sup Lee*

Department of Textile Engineering, INHA University, Incheon 402-751, Korea

Received July 26, 2005
Revised Manuscript Received September 9, 2005

Introduction

Since many properties of thin polymer materials are highly dependent on their surfaces and interfaces, a fundamental understanding of the influence of these factors on the structural aspects of polymers, such as their conformation,[1] dynamics,[2] and the local packing[3] of the polymeric chains, is essential in the case of thin polymer films. To optimize the performance of polymeric thin films, a number of structural parameters such as their orientation, conformation, and the crystalline structure of the polymer film at the surfaces, which are very difficult to deduce from the corresponding properties of the bulk materials, need to be carefully characterized.

The FTIR-ATR method is frequently used for the structural characterization of the surfaces of thick polymer films, fibers, and coatings because absorption occurs mainly at the surface of the sample. One of the most important aspects of the FTIR-ATR method is that, upon total internal reflection at the interface between the ATR crystal and sample, the electric field of the evanescent wave exists in all three spatial directions in the rarer medium (sample).[4] Therefore, it is possible to obtain orientation information along three spatial directions with the FTIR-ATR method.[5−10] The information we can obtain with FTIR-ATR is limited to the region within the penetration depth (0.1−10 μm) of the evanescent wave, which is determined by the wavelength of the incident infrared radiation, the incident angle, and the refractive indices of the ATR crystal and polymer sample.

Recently, grazing incidence X-ray diffraction (GIXRD) has attracted a great deal of interest due to its potential use for evaluating the crystalline structures which were hitherto difficult to analyze, such as the crystallinity and crystal orientation at the surface of a crystalline polymer.[11−17] Using this technique, the characteristic behavior of the polymer chains in the crystalline phase near the surface has been shown to be very different from that in the bulk. When using incidence angles smaller than the critical angle of the polymer sample employed, the scattered X-ray radiation contains information on the crystalline phase in the surface region within a few nanometers of the surface. Structural information on the crystalline phases within a few micrometers of the surface can also be obtained by using an angle of incidence larger than the critical angle.

Factor et al.[12] reported the surface-induced ordering of an aromatic polyimide which was measured using the GIXRD method. It was shown that within the first 90 Å from the surface the ordering of the polymer was markedly enhanced. In addition, the lateral registry of the molecules parallel to the surface of the film extended over relatively large distances of ∼150 Å. Surface-induced ordering during the crystallization of PET films was also reported.[17] Using GIXRD again, the ordering process was observed to occur at the free surface of PET when it was annealed at 80−90 °C. During the isothermal crystallization, the benzene rings in PET were found to be oriented preferentially with the ring plane parallel to the surface, and this ordering extended at least 1500 Å into the bulk of the specimen. The surface ordering of aliphatic chains was also observed in a molecular simulation study. Ito et al.[18] studied the crystallization of a free-standing thin film by means of the molecular dynamics simulation of a united atom model of PE in continuous space. Following the rapid quenching of a free-standing thin film from 500 to 300 K, crystals nucleated spontaneously, and independently, at both surfaces, with the long axis of the crystalline chains oriented in the plane of the thin film. The independently nucleated crystals grew by propagation into the interior of the thin film from both surfaces.

In this short report, the surface effect on the crystal orientation of cold crystallized poly(trimethylene 2,6-naphthalate) (PTN), which was recently introduced as a new material that has a high potential to be used as an engineering plastic, was investigated using temperature-controlled polarized FTIR-ATR and synchrotron-sourced GIXRD measurements. By comparing the results obtained using these two techniques, we were able to demonstrate the usefulness of the temperature-controlled polarized FTIR-ATR technique for the characterization of the surface orientation behavior.

Experimental Section

The PTN sample studied in this work showed an intrinsic viscosity of 0.52 dL/g measured in a mixed solvent of 1,1,2,2-tetrachloroethane and phenol (1/1, w/w) at 25 °C. To make the melt-quenched amorphous films for the FTIR-ATR measurement, PTN chips were pressed at 235 °C (T_m = 204 °C) for 3 min with a melt presser, followed by quenching into ice water. The film thickness was about 0.2 mm. The fact that the refractive indices along all three orthogonal directions measured with a polarized Abbe refractometer (Atogo, Abbe refractometer 4T) were almost identical indicates that the melt quenched film was isotropic[8,9] (data shown in Figure S1 in the Supporting Information). To make the thin films used for the GIXRD measurement, the samples were prepared by spin-coating them onto a silicon(100) wafer from a 3 wt % solution in 1,1,1,3,3,3-hexafluoro-2-propanol with a spinning speed of 1000 rpm. Uniform films with a thickness of about 700 nm were able to be obtained. Following spin-coating, the as-coated sample was baked in a vacuum oven at 40 °C for 12 h to remove the residual solvent. To remove any anisotropy that might be introduced by the high shear flow during spin-coating, the thin PTN film on the silicon wafer was heat-treated again at 235 °C (T_m = 204 °C) for 3 min followed by quenching into liquid nitrogen.

The FTIR-ATR spectra were obtained using the ATR setup developed initially by Sung,[7] which consists of a symmetrically double-edged parallelogram crystal and a rotatable sample holder. The ATR crystal was made of GaAs (n = 3.13 at 1000 cm^{-1}). The structural change which occurred during the heating process was studied directly while the sample was being heated inside the temperature-controlled polarized

* To whom all correspondence should be addressed. E-mail: hslee@inha.ac.kr.

10.1021/ma051651o CCC: $30.25
Published on Web 10/13/2005

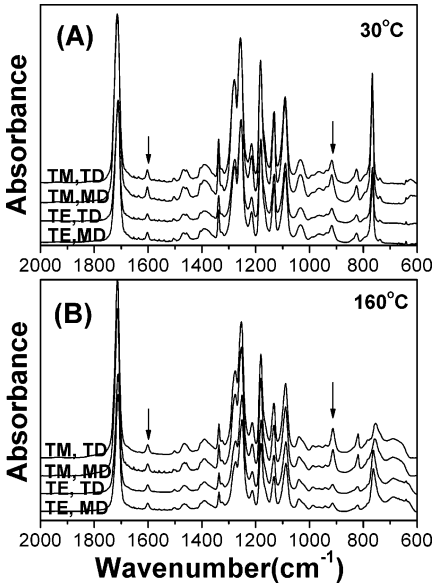

Figure 1. Raw ATR spectra at (A) 30 °C and (B) 160 °C obtained during the heating of the melt-quenched PTN film.

FTIR-ATR setup.[10] The orientation of the polymer segments at a certain temperature was estimated from the difference in absorbance of a specific infrared band in the four infrared spectra obtained at four different experimental geometries, using a procedure which is explained in detail in previous publications.[8−10] The GIXRD measurements were carried out in a vacuum chamber with a temperature-controlled sample stage and a 2D CCD detector installed at the 4C2 Beamline of the PAL (Pohang Accelerator Laboratory, Korea).[19] The wavelength of the incident X-rays was 1.54 Å.

Results and Discussion

Figures 1A,B shows a set of four ATR spectra obtained at 30 and 160 °C using four experimental geometries (TM/MD, TM/TD, TE/MD, and TE/TD). The samples in the ATR setup were heated stepwise to specific temperatures, and a set of four ATR spectra were collected at each temperature. The polarization mode (TE or TM) was determined by the polarization direction of the incident infrared radiation. The electric field direction of the TE mode is parallel with the surface of the films, whereas that of the TM mode consists of two electric components, i.e., parallel with as well as perpendicular to the film plane. Therefore, information on the surface-induced orientation can be obtained from the absorbance ratio of the selected band in the TM spectrum relative to the corresponding one in the TE spectrum (A_{TM}/A_{TE}).

The bands studied in this work are marked by arrows in Figure 1. The band at 1602 cm^{-1} is associated with the C=C stretching mode in the naphthalene ring, and its transition dipole moment is "parallel" to the naphthalene ring plane. The band at 917 cm^{-1} is related to the out-of-plane bending mode of the C−H bond in the naphthalene ring, and its transition dipole moment is "perpendicular" to the ring plane.[20,21] As can be seen from Figure 1A obtained at 30 °C, the absorbances of the 1602 and 917 cm^{-1} bands of the TM spectra (TM/MD or TM/TD) are significantly bigger than the corresponding ones of the TE spectra (TE/MD or TE/TD). When the temperature was increased to 160 °C, the absorbance of the 1602 cm^{-1} band in the TM spectra became comparable with that of the corresponding band in the TE spectra, whereas the absorbance of the 917 cm^{-1} band in the TM spectra became even greater than

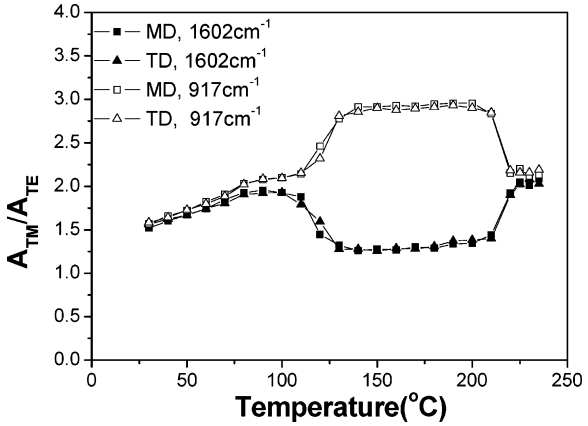

Figure 2. Absorbances of the 1602 (■, ▲) and 917 cm^{-1} (□, △) bands in the TM spectrum are divided by the corresponding ones in the TE spectrum, and the resulting ratios are plotted as a function of temperature.

that of the corresponding band in the TE spectra. This change in absorbance might be related to the surface-induced orientation of the crystals formed during the cold crystallization process which occurred at ∼110 °C.

The absorbance ratios (A_{TM}/A_{TE}) of the 1602 and 917 cm^{-1} bands are plotted as a function of temperature in Figure 2. Since the PTN films used for the ATR measurement were undrawn, the two mutually perpendicular directions (MD and TD) in Figure 2 were chosen arbitrary in the film plane. At room temperature, the absorbance ratios (A_{TM}/A_{TE}) of the two bands are almost identical. As the temperature increases from room temperature to the glass transition temperature of PTN ($T_g = 83$ °C), the absorbance ratios slowly increase, with no appreciable difference being observed between the two values. It is noted that the ratio becomes almost 2 at about 80 °C. As the temperature is increased above the cold crystallization value (about 110 °C), the ratios show an abrupt deviation from the value of 2, at which point the ratio of the 1602 cm^{-1} band decreases, while that of the 917 cm^{-1} band increases. As the temperature increases further above the melting transition ($T_m = 204$ °C), the ratios for both infrared bands reconverge and become close to 2 again.

The absorbance of a specific band obtained from the FTIR-ATR spectrum is affected not only by the orientation and quality of the optical contact between the sample and ATR crystal but also by the polarization direction of the incident IR radiation. The effective thickness for the TE and TM waves ($d_{e,TE}$, $d_{e,TM}$) can be calculated using the following equations:[4]

$$\frac{d_e(\mathrm{TE})}{\lambda_1} = \frac{n\cos\theta}{\pi(1-n^2)(\sin^2\theta - n^2)^{1/2}}$$

$$\frac{d_e(\mathrm{TM})}{\lambda_1} = \frac{n\cos\theta(2\sin^2\theta - n^2)}{\pi(1-n^2)[(1+n^2)\sin^2\theta - n^2](\sin^2\theta - n^2)^{1/2}}$$

$$\lambda_1 = \lambda/n_{\mathrm{crystal}};\quad n = \frac{n_{\mathrm{sample}}}{n_{\mathrm{crystal}}} \qquad (1)$$

As can be seen from eq 1, the effective thickness of both waves is a function of the refractive index of the sample, the angle of incidence, and the wavelength of the infrared radiation. Furthermore, the effective thickness of the TM wave ($d_{e,TM}$) is always greater than that of the TE wave ($d_{e,TE}$). When the angle of incidence is 45°,

the effective thickness ratio ($d_{e,TM}/d_{e,TE}$) of the two waves is 2 for any isotropic sample, as can easily be confirmed using eq 1. This means that the ratio of the two absorbances (A_{TM}/A_{TE}) should become 2, provided that the contact between the sample and ATR crystal is perfect. The absorbance ratio of about 1.5 observed at room temperature in Figure 2 is, therefore, due to the nonideal optical contact between the PTN sample in the glassy state and ATR crystal. However, the identical ratio values of the 1602 and 917 cm^{-1} bands indicate that the melt-quenched PTN film is in the isotropic state. The fact that the ratio becomes close to 2 at temperatures near T_g suggests that the optical contact becomes almost ideal at this temperature. As the temperature increases further above T_g, cold crystallization occurs. The temperature at which an abrupt deviation from 2 is observed corresponds to the cold crystallization phenomenon that was confirmed in the DSC scan and wide-angle X-ray scattering experiments (data shown in Figures S2 and S3 in the Supporting Information). The sudden decrease/increase in the A_{TM}/A_{TE} values of the 1602 and 917 cm^{-1} bands can be explained in terms of the surface-induced in-plane orientation of the naphthalene rings in the crystal formed during the cold-crystallization process. As the naphthalene ring tends to orient in the film surface, the absorbance of the 1602 cm^{-1} band in the TM spectra becomes smaller, while that in the TE spectra becomes bigger, resulting in an abrupt decrease in the absorbance ratio (A_{TM}/A_{TE}). Since the transition moment of the band at 917 cm^{-1} is "perpendicular" to the ring plane, the behavior of the ratio for this band is opposite to that of the ratio for the 1602 cm^{-1} band, as shown in Figure 2. As the temperature increases further up to the melting transition (T_m = 204 °C), the ratios for both infrared bands become close to 2, which is a clear indication of the transition to the isotropic state upon melting. On the basis of the results shown in Figure 2, it might be concluded that the cold crystallization process of PTN induces the in-plane orientation of the naphthalene rings, at least in the surface region within about 1 μm of the film surface. (The penetration depths of the 1602 and 917 cm^{-1} bands are approximately 0.67 and 1.17 μm, respectively.)

Figure 3A shows the WAXD profile of the cold-crystallized PTN film (~0.2 mm thickness) annealed at 160 °C obtained using the transmission WAXD method. PTN is known to have two crystal structures, i.e., the α and β forms. The α crystal structure can be obtained by cold-crystallization (low-temperature crystallization), whereas the β crystal structure is obtained by melt crystallization (high-temperature crystallization). The α-form PTN crystal was reported to have a monoclinic crystal system with unit cell parameters of a = 0.722 nm, b = 0.709 nm, c = 2.384 nm, α = 90.0°, β = 90.0°, and γ = 81.6°.[22] Although the detailed chain structure in a unit cell of the PTN β crystal has previously been reported, the chain conformation in the α-form crystal has not been reported yet.[23] As expected from the cold crystallization processing, it is clear that the α-form crystal structure of PTN was formed, and the assignments of the diffraction peaks are included in Figure 3A.

Two-dimensional GIXRD profiles of cold-crystallized PTN film were obtained at 160 °C using various incidence angles between 0.12° and 0.22° that were both below and above the critical angles (the critical incidence angle of PTN is 0.17°). The general features of GIXRD profiles were maintained over the angle ranges studied. Figure 3B shows the two one-dimensional GIXRD profiles ((1) out-of-plane scan, (2) in-plane scan) of the cold-crystallized PTN film obtained using an incidence angle of 0.18°. The two-dimensional scattering pattern is shown in the small inset. By comparing this result with the profile in Figure 3A, we can easily confirm that the crystal structure observed in Figure 3B is the α-form. However, the relative intensity of each diffraction peak in the out-of-plane scan is quite different from that of the corresponding peak in the in-plane scan profile. In the case of the out-of-plane scan, the intensity of the (201) plane reflection is much stronger, and the intensities of the (011), (012), and (013) plane reflections were much weaker than the corresponding peaks in the in-plane scan profile. These results clearly indicate that the crystal formed during the cold crystallization process is anisotropic. The reflection from the (002) plane was observed only in the in-plane scan profile. This result means that the "a" axis of the monoclinic unit cell is preferentially orientated almost perpendicular to the film plane, at least up to a depth of several micrometers from the surface. The higher intensity of the (0kl) crystal planes in the in-plane scan is also indicative of the nonisotropic crystal orientation suggested above. If the "a" axis is perfectly perpendicular to the film plane, the c axis becomes parallel with the film plane while the b axis is slightly skewed (about 8.4°) from the film plane.[22] The higher intensity of the (201) plane in the out-of-plane scan is also to be expected if the "a" axis is "perpendicular" to the film plane.

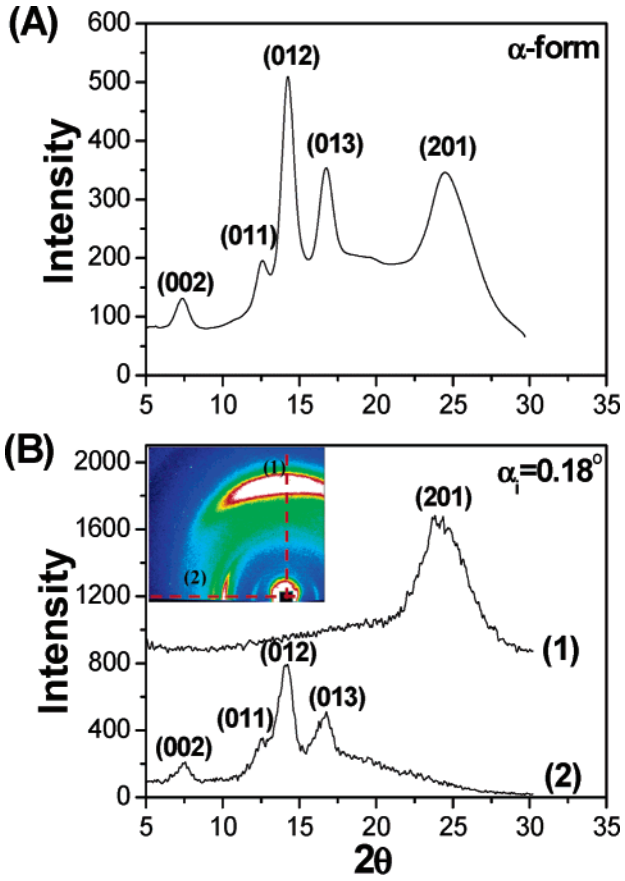

Figure 3. (A) WAXD profile of PTN with α-form crystals. (B) Out-of-plane scan profile (1) and in-plane scan profile (2) obtained from 2D GIXRD patterns shown in the small inset.

The GIXRD results indicate that the "*a*" axis is almost perpendicular to the film surface, while the two other axes ("*b*" and "*c*") are more parallel. It was confirmed from the FTIR-ATR results that the naphthalene ring in the crystal phase formed during the cold crystallization process was "parallel" with the film surface. Therefore, the GIXRD results shown in Figure 3B suggest that the naphthalene ring plane is approximately parallel with the "*bc*" plane of the PTN crystal that was formed. As mentioned above, the detailed chain structure in the α-form has not been reported yet. However, the ring plane normal in the β-form PTN crystal is known to deviate from the "*bc*" plane normal by 10.2°.[23] It can therefore be concluded that the ring plane in the α-form PTN is almost "parallel" with the "*bc*" crystal plane, as in the case of the β-form crystal.

Conclusions

In this work, the surface-induced crystal orientation behavior of PTN formed during the cold crystallization process was analyzed with polarized FTIR-ATR spectroscopy and GIXRD using synchrotron X-ray radiation. It was found that polarized FTIR-ATR can be a convenient tool to demonstrate the anisotropic surface orientation of the chain segments, and the results were confirmed on the basis of the difference between the out-of-plane and in-plane scan profiles obtained from the two-dimensional GIXRD patterns. The anisotropic distribution of the naphthalene rings in the PTN crystal in the surface region appears to be due to the surface effect on the crystallization process. The preferential orientation of the naphthalene rings in the crystalline phases formed during the cold crystallization process can be explained in terms of the surface-induced nucleation followed by crystal growth along the normal direction away from the surface. The orientation of the naphthalene rings near the surface (probably up to a depth of several nanometers from the surface), which is not readily detected in the FTIR-ATR results shown in Figure 2, can initiate the nucleation process, and the surface-induced orientation can be further amplified by the crystal growth process. If the nucleation starts at a position far away from the surface, there is no obvious reason for surface-related orientation to occur. From the X-ray diffraction pattern of the cold-crystallized PTN films obtained by illuminating the X-rays into the plane, as well as the side, of the films, we could not observe any definite oriented structure (data shown in Figure S4 in the Supporting Information). This result indicates that the anisotropic orientation shown in Figure 2 is confined to a maximum depth of several micrometers below the surface. Since most of the nuclei are formed far away from the surface, thick PTN films with thicknesses of several millimeters do not show any anisotropic orientation of the crystal.

Acknowledgment. This work was supported by an INHA University Research Grant. The X-ray experiments at PLS, Korea, were supported by MOST and POSCO, Korea.

Supporting Information Available: Figures showing principal refractive indices as a function of draw ratio (S1), DCS thermogram of melt-quenched PTN film (S2), WAXD profiles obtained during melt-quenched PTN film (S3), and 2D WAXS pattern of melt-quenched and annealed PTN film (S4). This material is available free of charge via the Internet at http://pubs.acs.org.

References and Notes

(1) Vacatello, M. *Macromol. Theory Simul.* **2001**, *10*, 198−195.
(2) Kerle, T.; Lin, Z.; Kim, H.-C.; Russell, T. P. *Macromolecules* **2001**, *34*, 3484−3492.
(3) Yakabe, H.; Tanaka, K.; Nagamura, T.; Sasaki, S.; Sakata, O.; Takahara, A.; Kajiyama, T. *Polym. Bull. (Berlin)* **2005**, *53*, 213−222.
(4) Harrick, N. J. *Internal Reflection Spectroscopy*; Interscience Publishers; John Wiley & Sons: New York, 1967.
(5) Flournoy, P. A.; Schaffers, W. J. *Spectrochim. Acta* **1966**, *22*, 5−13.
(6) Flournoy, P. A. *Spectrochim. Acta* **1966**, *22*, 15−20.
(7) Sung, C. S. P. *Macromolecules* **1981**, *14*, 591−594.
(8) Lee, H. S.; Park, S. C.; Kim, Y. H. *Macromolecules* **2000**, *33*, 7994−8001.
(9) Park, S. C.; Liang, Y.; Lee, H. S. *Macromolecules* **2004**, *37*, 5607−5614.
(10) Park, S. C.; Liang, Y.; Lee, H. S.; Kim, Y. H. *Polymer* **2004**, *45*, 8981−8988.
(11) Factor, B. J.; Russell, T. P.; Toney, M. F. *Macromolecules* **1993**, *26*, 2847−2859.
(12) Factor, B. J.; Russell, T. P.; Toney, M. F. *Phys. Rev. Lett.* **1991**, *66*, 1181−1184.
(13) Toney, M. F.; Russell, T. P.; Logan, J. A.; Kikuchi, H.; Sands, J. M.; Kumar, S. K. *Nature (London)* **1995**, *374*, 709−711.
(14) Kawamoto, N.; Mori, H.; Nitta, K.; Sasaki, S.; Yui, N.; Terano, M. *J. Chem. Phys.* **1998**, *199*, 261−266.
(15) Macdonald, J. M.; Durell, M.; Trolley, D.; Lei, C.; Das, A.; Jukes, P. C.; Geoghegan, M.; Higgins, A. M.; Jones, R. A. L. *Radiat. Phys. Chem.* **2004**, *71*, 811−815.
(16) Jukes, P. C.; Das, A.; Durell, M.; Trolley, D.; Higgins, A. M.; Geoghegan, M.; Macdonald, J. E.; Jones, R. A. L.; Brown, S.; Thompson, P. *Macromolecules* **2005**, *38*, 2315−2320.
(17) Durell, M.; Macdonald, J. M.; Trolley, D.; Wehrum, A.; Jukes, P. C.; Jones, R. A. L.; Walker, C. J.; Brown, S. *Europhys. Lett.* **2002**, *58*, 844−850.
(18) Ito, M.; Matsumoto, M.; Doi, M. *Fluid Phase Equilib.* **1998**, *144*, 395−401.
(19) Pohang Accelerator Laboratory, http://pal.postech.ac.kr/eng.
(20) Stier, U.; Oppermann, W. *J. Polym. Sci., Part A: Polym. Chem.* **2001**, *39*, 620−629.
(21) Ouchi, I.; Hosoi, M.; Shimotsuma, S. *J. Appl. Polym. Sci.* **1977**, *21*, 3445−3456.
(22) Jeong, Y. G.; Jo, W. H.; Lee, S. C. *Polymer* **2003**, *44*, 3259−3267.
(23) Jeong, Y. G.; Jo, W. H.; Lee, S. C. *Polymer* **2004**, *45*, 379−384.

MA051651O